ATMOSPHERIC SCIENCE LETTERS
Atmos. Sci. Let. **18**: 29–36 (2017)
Published online 19 December 2016 in Wiley Online Library
(wileyonlinelibrary.com) **DOI:** 10.1002/asl.720

RMetS
Royal Meteorological Society

Multidecadal convection permitting climate simulations over Belgium: sensitivity of future precipitation extremes

Sajjad Saeed,[1,5]* Erwan Brisson,[2] Matthias Demuzere,[1] Hossein Tabari,[3] Patrick Willems[3,4] and Nicole P. M. van Lipzig[1]

[1]*Department of Earth and Environmental Sciences, KU Leuven, Belgium*
[2]*Goethe University, Frankfurt, Germany*
[3]*Hydraulics Division, Department of Civil Engineering, KU Leuven, Belgium*
[4]*Department of Hydrology and Hydraulic Engineering, Vrije Universiteit Brussel, Belgium*
[5]*Center of Excellence for Climate Change Research (CECCR), King Abdulaziz University, Jeddah, Saudi Arabia*

**Correspondence to:*
S. Saeed, Department of Earth and Environmental Sciences, Celestijnenlaan 200e – box 2409, BE-3001 KU Leuven, Leuven, Belgium.
E-mail: sajjad.saeed@kuleuven.be

Received: 26 February 2016
Revised: 16 November 2016
Accepted: 17 November 2016

Abstract

We performed five high resolution (2.8 km) decadal convection permitting scale (CPS) climate simulations over Belgium using the COSMO-CLM regional climate model and examined the future changes in daily precipitation extremes compared to coarser resolution simulations. The CPS model underestimates the higher percentiles during both seasons, however, some improvements in the higher percentile values are noticed during the summer season. Analysis of three future climate simulations indicates that the CPS model modifies the future signals of daily precipitation extremes compared to their forcing non-CPS simulations during summer. During this season, the increase (decrease) in the daily precipitation extremes is stronger in the CPS compared to the non-CPS simulations. During winter, no significant changes between CPS and non-CPS were found.

Keywords: **regional climate model; convection permitting simulations; extreme precipitation**

1. Introduction

Extreme precipitation events largely influence society and ecosystems through floods, drought, infrastructure damage and even human causalities (Tabari *et al.*, 2014). According to the 5th assessment report (AR5) of the International Panel on Climate Change (IPCC), the frequency and intensity of the precipitation extremes are likely to increase in the future warmer climate (IPCC, 2013). Understanding and quantifying the magnitude and frequency of such extremes for both the present-day climate and possible future climates is therefore relevant. IPCC's future climate projections are generally based on coarser resolution (e.g. 150–200 km or more) Global Climate Model simulations. Owing to their coarse resolution, not all processes, notably those occurring on mesoscales, are reasonably taken into account. These limitations result in important misrepresentations of extreme precipitation (Willems *et al.*, 2012; Tabari *et al.*, 2015).

To overcome this problem, Regional Climate Models (RCMs) are frequently used to downscale the coarser resolution global climate simulations to regional and local scales. The RCMs are capable of providing additional regional details such as an improved representation of topographical features (e.g. mountains and coastlines), land cover heterogeneity etc. (Christensen and Christensen, 2007; Prein *et al.*, 2015). The recent internationally coordinated projects, e.g. PRUDENCE, ENSEMBLES and EURO-CORDEX employed RCMs with horizontal resolutions of 50, 25 and 12 km, respectively (Christensen and Christensen, 2007; Mearns *et al.*, 2009; Kotlarski *et al.*, 2014). Some recent studies performed climate simulations even at 7 km spatial resolution (Wagner *et al.*, 2013). The increasing model resolution, however, does not guarantee a reduction of the model deficiencies and associated biases compared to the observations. Some studies (Clark *et al.*, 2007; Walther *et al.*, 2013) indicate that the increasing model resolution does not improve the representation of the precipitation diurnal cycle. This problem has been solved partly by resolving deep convection, a process that can be modeled in RCMs with grid mesh size as fine as at least 2–4 km (Weisman *et al.*, 1997). Such high resolution RCM simulations where deep convection is explicitly resolved are generally referred as convective permitting scale (CPS) simulations. Previous studies (Kendon *et al.*, 2012; Prein *et al.*, 2013; Ban *et al.*, 2014; Fosser *et al.*, 2014; Brisson *et al.*, 2016) showed that CPS models improve the representation of the diurnal cycle of precipitation. However, due to the high computational cost of CPS models, the number of climate change impact studies using such models is limited (Prein *et al.*, 2015).

In most studies discussed above, the CPS model simulations are carried out to investigate their added value in the present-day climate. Only few studies examined future precipitation extremes in the CPS model simulations (Kendon *et al.*, 2014; Ban *et al.*, 2015). The latter two studies slightly disagree in their findings due to use of different statistical methods (Schär *et al.*, 2016). Kendon *et al.* (2014) noticed a future intensification of

short-duration rain in summer, with significantly more events exceeding the high thresholds. Whereas, Ban *et al.* (2015) showed that the extreme events are projected to become more frequent and more intense, but not as pronounced as in some previous studies. Additional simulations are therefore needed to investigate the reasons for diverging conclusions in these recent studies. This study aims to fill this gap by performing a set of present-day and future decadal CPS simulations over Belgium. Among other issues, an important question remains: how do high resolution CPS model integrations modify the representation of future precipitation extremes compared to the non-CPS simulations? The advantage of this study is that it relies on three separate 10-year future climate simulations, which makes it possible to study the robustness of the signals. The article is organized as follows: The next section gives an overview of the COSMO-CLM (CCLM) model and the configuration of the CPS simulations. A brief model evaluation and the simulated future changes in the precipitation extremes are described in the Section on Results and Discussions. The summary and conclusions are presented in the last section.

2. Data and methodology

2.1. Model

This study uses the CCLM RCM, a non-hydrostatic model based on the COSMO numerical weather prediction model (Steppeler *et al.*, 2003). Later on, the model was adapted by the climate limited-area modeling (CLM) community to perform both short- and long-term climate integrations by adding specific modules such as dynamic surface boundaries, a more complex soil model and the possibility to use various CO_2 concentrations (Böhm *et al.*, 2006; Rockel *et al.*, 2008).

Following Brisson *et al.* (2016), here we adopt the third order Runga-Kutta split-explicit time stepping scheme (Wicker and Skamarock, 2002), the lower boundary fluxes provided by the TERRA model (Doms *et al.*, 2011) and the radiative scheme after Ritter and Geleyn (1992). In this respect, it is noted that the precipitation change might be adversely affected by some deficiencies shortwave water vapor absorption in older radiative transfer schemes (DeAngelis *et al.*, 2015).

2.2. Experimental setup and methodology

The experimental setup in terms of model domains, physical parameterizations etc. generally follows that of Brisson *et al.* (2016). A three-step nesting strategy (shown in Figure S1) has been applied in this study. Five simulations are performed (Table S1). For simplicity, here LTS refers to the long-term simulation and the subscript represents the lateral boundary conditions. The ERA-Interim reanalysis data and the global EC-Earth model (Dee *et al.*, 2011; Hazeleger *et al.*, 2012) provides the necessary initial and boundary conditions to nest a 100×100 grid points domain with a 0.22° (approximately 25 km) grid mesh size. The resulting 3-h outputs are employed to nest a 0.0625° (approximately 7 km) domain. Finally, the hourly outputs of the latter nest, characterized by 150×150 grid points, are used as input for the 0.025° (approximately 2.8 km) simulation on a 192×175 grid points domain. The added value of CPS can best be assessed when the model is driven with ERA-Interim boundary conditions ($LTS_{ERA\text{-}Int}$), as deficiencies in the EC-Earth model might propagate into the regional model. The non-CPS model with horizontal resolutions of 25 and 7 km does not explicitly resolve deep convection and hence use the convection scheme after Tiedtke (1989). Such parameterization is unnecessary in the CPS (2.8 km) model setup where deep convection is dynamically resolved.

Table 1. Definition of indices used in this study.

Index	Definition
Wet days	Days for which daily precipitation exceeds 90th percentile of reference period
Very wet days	Days for which daily precipitation exceeds 95th percentile of reference period
Extreme wet days	Days for which daily precipitation exceeds 99th percentile of reference period
Heavy rainfall	The mean of the upper 5% of daily precipitation intensities
Extreme event	Daily precipitation over a particular grid cell exceeding 30 mm day^{-1}
Very extreme event	Daily precipitation over a particular grid cell exceeding 60 mm day^{-1}

All simulations performed in this study employ 40 vertical levels. Observational data for daily accumulated precipitation for 199 stations covering the full simulation period (2001–2010) obtained from the Royal Meteorological Institute (RMI) of Belgium are employed to evaluate the model in present-day climate. In the case of comparison with station data, we extracted model information from the nearest grid point. This method is commonly used for model and station data comparison but it may introduce some uncertainties as the model data are grid averaged values whereas the station data present point values. Several indices (Chan *et al.*, 2013; Ban *et al.*, 2015) that are used here are summarized in Table 1. The precipitation percentiles are computed from continued time series, which also includes dry days. To compare data on different grids, the simulated datasets are first regridded to 0.22° regular grid using conservative first order regridding method. This regridding method is more desirable than the bilinear interpolation for discontinuous variables such as precipitation (Jones, 1999).

3. Results and discussions

3.1. Present-day analysis

Brisson *et al.* (2016) performed a detailed evaluation of CCLM over Belgium driven with ERA-Interim

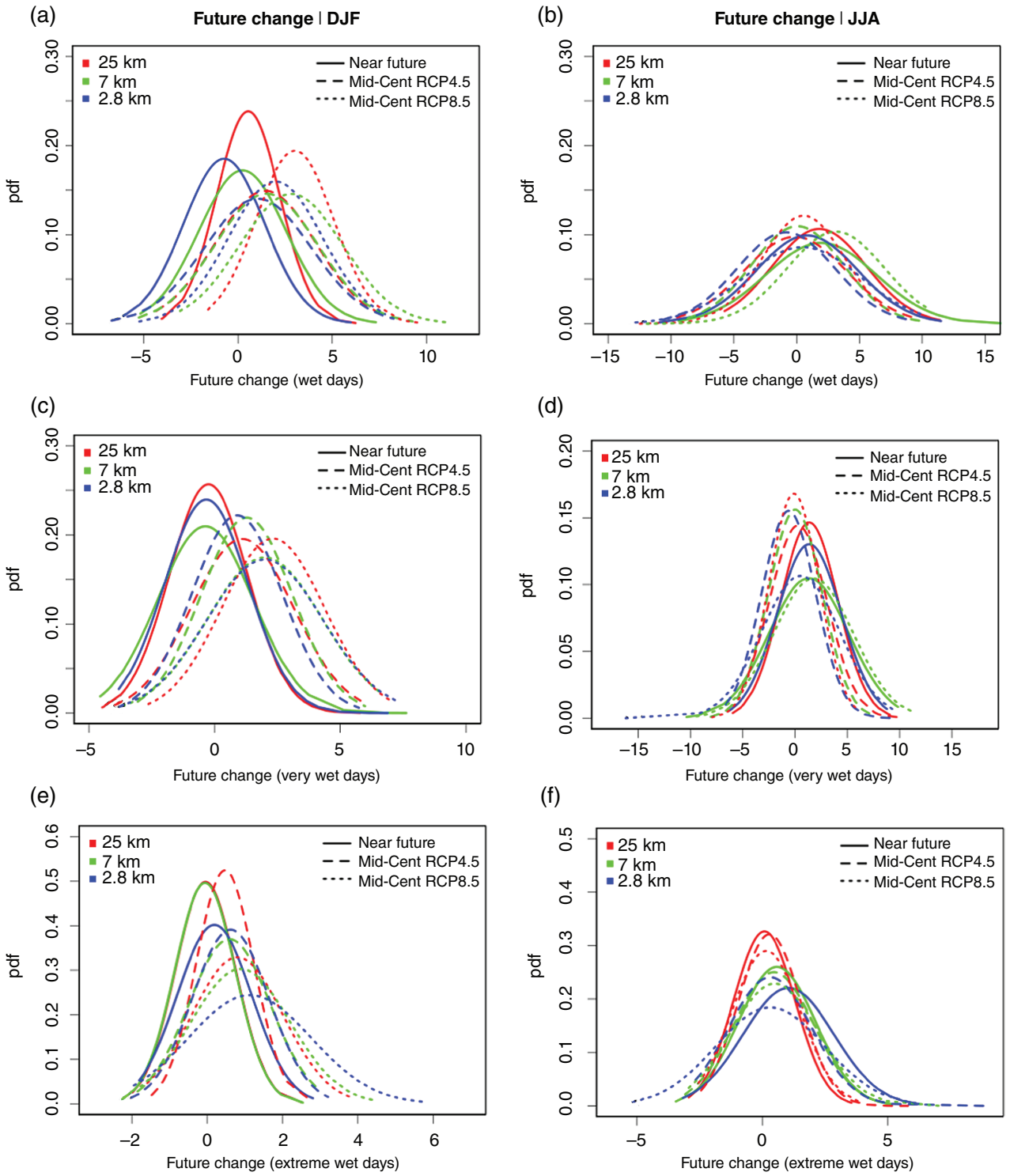

Figure 1. Future change in the wet, very wet and extreme wet days. The future changes are shown for Near Future (2026–2035) and Mid-Century (2060–2069) with respect to the present-day (2001–2010) period. In each case, the blue (red, green) lines show the CPS (non-CPS) model simulations.

boundary conditions. In this study we extend this evaluation for present-day simulation driven by EC-Earth boundary conditions ($LTS_{EC\text{-}Earth}$, Table S1). Table S2 gives the mean and higher percentiles for winter and summer for the set of present-day simulations ($LTS_{ERA\text{-}Int}$ and $LTS_{EC\text{-}Earth}$). Note that, due to the sparse network of station data it was not possible to aggregate the observations to a grid. The model data is not area averaged, it just consists of all points and dates for which there exists a station in the RMI database. Compared to the observations the CPS model underestimates the higher percentiles during both seasons, however, some improvements in the higher percentile values are noticed during the summer season. This is especially evident for the $LTS_{ERA\text{-}Int}$ run. For the $LTS_{EC\text{-}Earth}$ simulation, the CPS model does not show

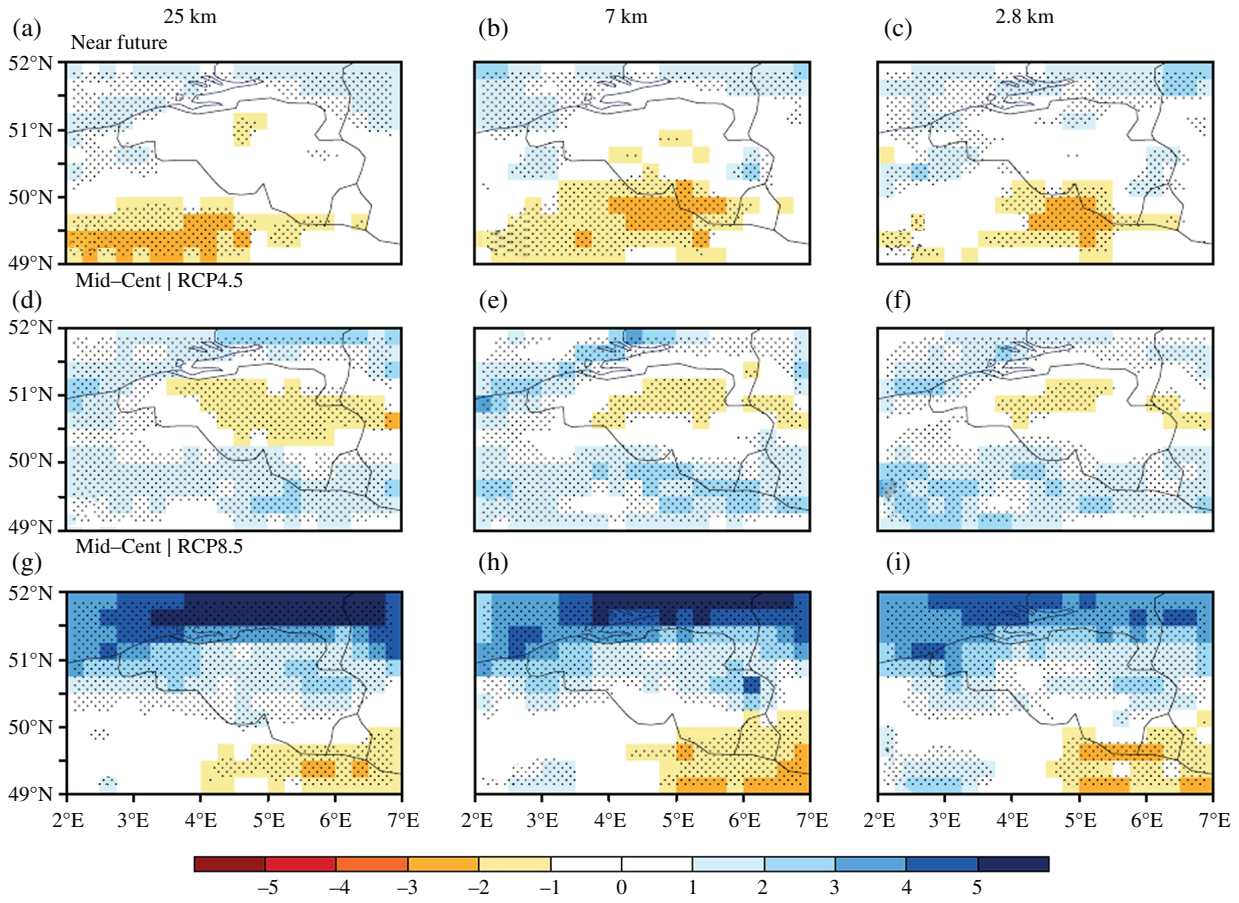

Figure 2. Future change in heavy precipitation (mm day^{-1}) during winter season. Similar to Figure 1, the future changes are computed for Near Future (2026–2035) and Mid-Century (2060–2069) with respect to the present-day (2001–2010) period. The left two panels show future changes for the non-CPS model simulations whereas the right panel show the future changes for CPS model simulations. The model resolutions are shown on the top of panel. The dotted areas indicate differences that are significant at 99% confidence level based on *t*-test.

marked improvements or deteriorations compared to the non-CPS simulations, at least not on a daily time scale.

3.2. Future simulation of extreme precipitation over Belgium

The main aim of this article is to investigate the CPS model response to increasing greenhouse gas forcing compared to non-CPS models. We therefore first examine the future change in number of simulated wet, very wet and extreme wet days as defined in Table 1. For this purpose, we computed for each grid cell the change in number of days for each category between the future and the present-day. We then constructed a sample consisting of these change values for each grid cell. In the final step, we examined the spatial distribution of future change in wet, very wet and extreme wet days (Figure 1). The most robust signal is found for extreme wet days where all three CPS simulations show an amplification of the future signals for both seasons compared to the non-CPS simulations (Figures 1(e) and (f)). During the summer season, the extreme wet days show a wider distribution in the CPS model simulations (Figure 1(f)). In this season, the enhancement (reduction) in the future extreme wet days is more pronounced in all three CPS simulations compared to the non-CPS simulations. Note that the CPS model simulations also reveal a slight reduction in number of future wet and very wet days compared to the non-CPS simulations during both seasons (Figures 1(a)–(d)).

We further examine the intensity of future change in the heavy rainfall. During the winter season, both the CPS and non-CPS model simulations reveal a similar future change in the spatial distribution of heavy rainfall intensity over Belgium (Figure 2). Although, the area showing negative future change in heavy rainfall in the non-CPS model (Figures 2(a), (b), (d), (e), (g) and (h)) diminishes in the CPS model simulations (Figures 2(c), (f) and (i)), the difference between CPS and non-CPS is marginal during winter.

During summer, the CPS model simulations show amplification in the future signals of the heavy rainfall over Belgium compared to the non-CPS model simulations (Figures 3 and 4). Significant differences between CPS and non-CPS are found over some regions where precipitation increase (decrease) is stronger in the CPS compared to non-CPS simulations. However, some grid cells display minor changes in the simulated

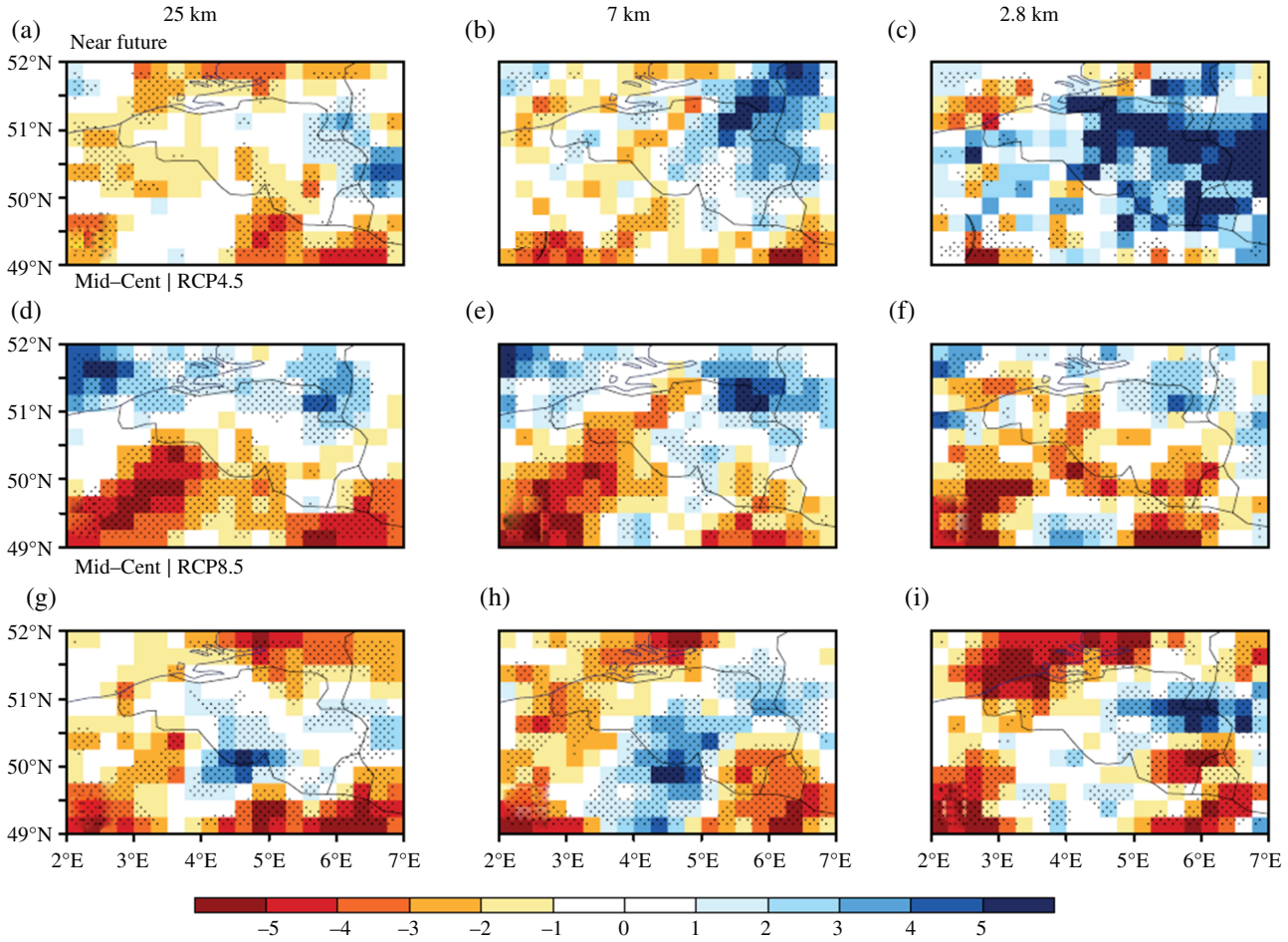

Figure 3. Same as Figure 2, but for summer season. The dotted areas indicate differences that are significant at 99% confidence level based on *t*-test.

patterns between CPS and non-CPS during the summer season (Figure 4). Based on the *t*-test, the regression coefficients for all these three simulations are significantly (99% level) different from one, hence rejecting the null hypothesis that both CPS and non-CPS have the same changes in heavy rainfall (Figure 4). Moreover, the slope of the regression lines between CPS (*x*-axis) and non-CPS (*y*-axis) is significantly (99% level) lower than 1 for all three simulations, indicates that the amplitude of the change, whether positive or negative, is significantly larger in CPS compared to the non-CPS (Figure 4).

We further examined the extreme and very extreme precipitation events (Table 1) by analyzing a cumulative distribution of the daily rainfall over Belgium (Figure 5). Each day and grid cell is treated as a sample of the distribution, so in total, the sample consists of the grid points in the analysis domain (198) multiplied with the number of days in the simulation (902 for winter and 920 for summer, yielding 178 596 values for winter and 182 160 values for summer). The cumulative distribution is plotted only for that part of the sample with daily rainfall rates above the threshold (30 and 60 mm day^{-1} respectively for very wet and extreme wet days). The upper limit of the precipitation imposed to define the daily extreme and

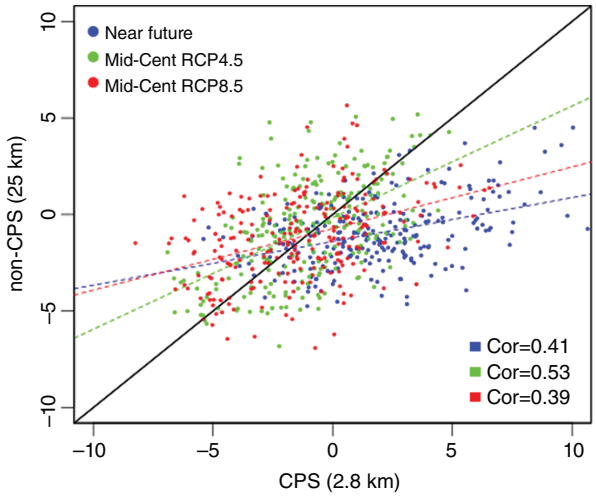

Figure 4. Scatter plot between CPS and non-CPS (25 km) simulated future change signal of heavy rainfall (mm day^{-1}) averaged over all summer seasons. Each dot in the scatter plot refers to a model grid cell. The blue, green and red dots show the change for Near Future, Mid-Cent$_{RCP4.5}$ and Mid-Cent$_{RCP8.5}$ simulations. The dashed blue, green and red lines indicate the regression lines for above three simulations respectively. The solid black line represents the (1 : 1) line. The correlation coefficients between CPS and non-CPS future change signals are significant to 95% level in all three cases and are shown in the lower left corner of the panel.

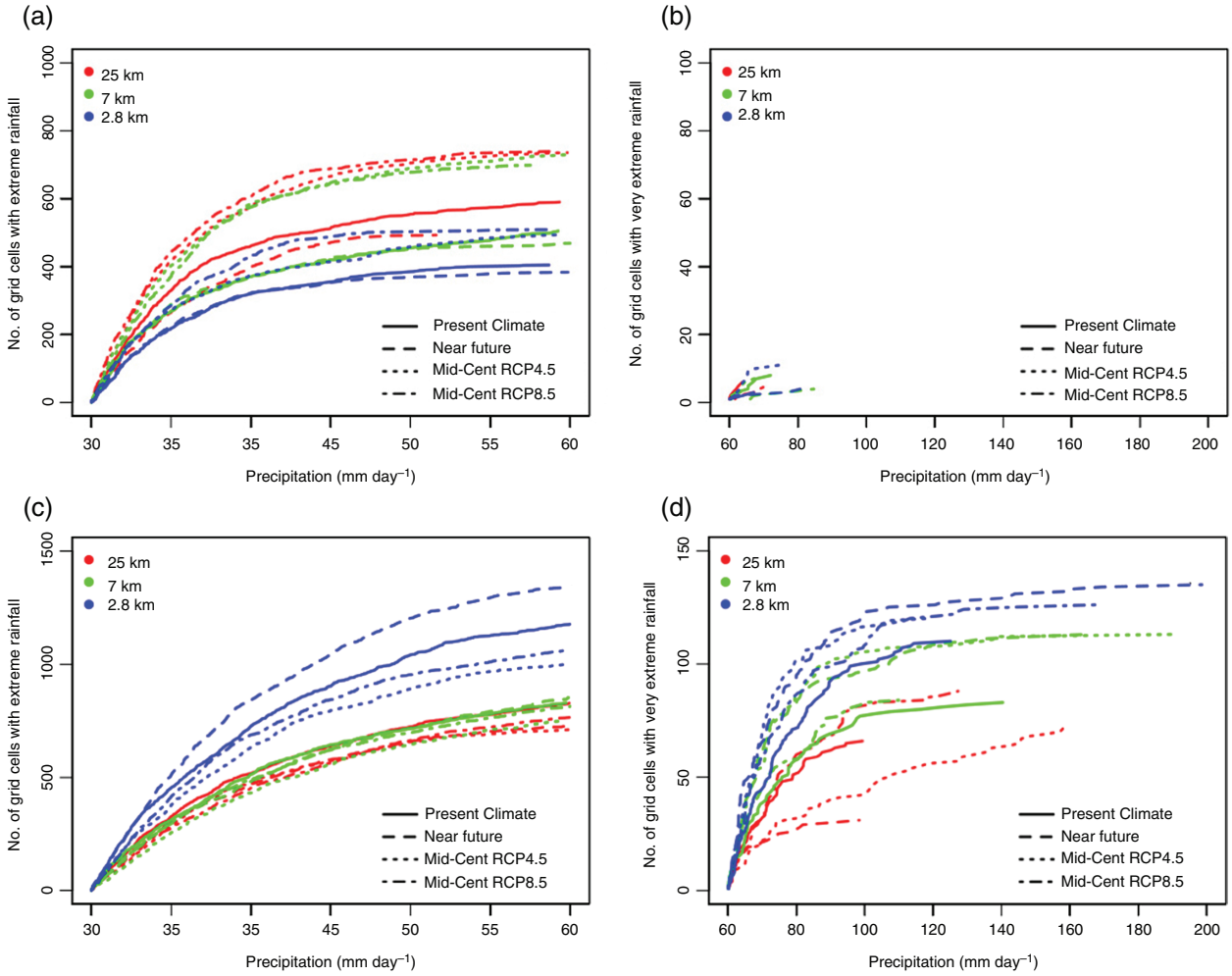

Figure 5. Cumulative distribution of the simulated daily precipitation extreme (a and c) and very extreme (b and d) events (mm day^{-1}) over Belgium during winter (a and b) and summer (c and d). The climate simulations performed in this study (Table S1) are represented by the solid, dashed, dotted and dot-dashed lines. In all cases, the blue (red, green) lines show the CPS (non-CPS) simulations.

very extreme events (in this case) is subjective and a small variation in this limit does not affect the overall results (not shown). During the winter season, neither CPS nor non-CPS simulations show robust signals between all three future simulations at grid cell scale (Figures 5(a) and (b)). However, during summer, both the frequency and intensity of the daily precipitation extremes covering a grid cell area also increase notably in the CPS simulations compared to the forcing non-CPS simulations (Figures 5(c) and (d)). Note that very high extremes are reached only in a very limited number of cases, while lower intensities are exceeded more frequently. The Near Future (Mid-Cent RCP4.5 and RCP8.5) CPS simulation has more (less) extreme compared to the present-day CPS (Figure 5(c)). We do not know the exact reason for this but since the last two simulations cover a different decade (2060–2069), there might be some decadal climate variability in the global model simulations that influence the RCM simulation results. However, for very extreme events (Figure 5(d)), there is clear amplification in the future signals in all cases compared to the present-day CPS simulation.

4. Summary and conclusions

The sensitivity of the future precipitation extremes on the daily time scale have been compared between the CPS simulations and their forcing non-CPS simulations. For this purpose, we performed five decadal high resolution (2.8 km) convection permitting scale (CPS) climate simulation over Belgium using the CCLM RCM. A detailed evaluation of the CCLM has been carried out by Brisson *et al.* (2016). This follow-up study assesses how the high resolution CPS model integrations may modify future signals of the daily precipitation extremes over Belgium compared to their forcing non-CPS simulations.

The analysis of three future simulations over Belgium with reference to the present-day climate reveals an amplification of the future daily precipitation extremes in the CPS simulations compared to the non-CPS simulations, both in frequency and intensity. This amplification is larger during the summer season. During winter, the difference between CPS and non-CPS is marginal. On the other hand, during the summer season, some regions where daily precipitation

extremes increase (decrease) in the forcing non-CPS simulations, they increase (decrease) more in the CPS simulations.

Acknowledgements

The authors thank two anonymous reviewers for helpful and insightful comments. This research has been carried out under the MACCBET and CORDEX-BE projects. MACCBET and CORDEX-BE are funded by the Belgian Science Policy (BELSPO). M.D. is funded by the Flemish regional government through a contract as a FWO (Fund for Scientific Research) post-doctoral position. The computational resources and services used in this work were provided by the VSC (Flemish Supercomputer Center), funded by the Hercules Foundation and the Flemish Government department EWI.

Supporting information

The following supporting information is available:

Figure S1. Model domains used for 25, 7 and 2.8 km resolution simulations. The analysis domain is shown by the red rectangle.

Table S1. Simulations performed in this study with COSMO-CLM regional climate model.

Table S2. Daily precipitation intensity spatio-temporal average, 95th and 99th quantiles for the observation and the different simulations for the winter and the summer period. The model data was extracted from the COSMO-CLM grid cells, which encompasses the coordinates of the Royal Meteorological Institute's observations (RMI-OBS) locations.

References

Ban N, Schmidli J, Schär C. 2014. Evaluation of the convection-resolving regional climate modeling approach in decade-long simulations. *Journal of Geophysical Research. Atmospheres* **119**(13): 7889–7907.

Ban N, Schmidli J, Schär C. 2015. Heavy precipitation in a changing climate: does short-term summer precipitation increase faster? *Geophysical Research Letters* **42**: 1165–1172.

Böhm U, Kücken M, Ahrens W, Block A, Hauffe D, Keuler K, Rockel B, Will A. 2006. CLM – the climate version of LM: brief description and long-term applications. *COSMO Newsletter* **6**: 225–235.

Brisson E, Van Weverberg K, Demuzere M, Devis A, Saeed S, Stengel M, van Lipzig NPM. 2016. How well can a convection-permitting climate model reproduce decadal statistics of precipitation, temperature and cloud characteristics? *Climate Dynamics* **47**: 3043–3061, doi: 10.1007/s00382-016-3012-z.

Chan SC, Kendon EJ, Fowler HJ, Blenkinsop S, Ferro CAT, Stephenso DB. 2013. Does increasing the spatial resolution of a regional climate model improve the simulated daily precipitation? *Climate Dynamics* **41**: 1475–1495.

Christensen JH, Christensen OB. 2007. A summary of the PRUDENCE model projections of changes in European climate by the end of this century. *Climatic Change* **81**: 7–30.

Clark AJ, Gallus WA, Chen TC. 2007. Comparison of the diurnal precipitation cycle in convection-resolving and non-convection-resolving mesoscale models. *Monthly Weather Review* **135**(10): 3456–3473.

DeAngelis AM, Qu X, Zelinka MD, Alex Hall A. 2015. An observational radiative constraint on hydrologic cycle intensification. *Nature* **528**: 249–253, doi: 10.1038/nature15770.

Dee DP, Uppala SM, Simmons AJ, Berrisford P, Poli P, Kobayashi S, Andrae U, Balmaseda MA, Balsamo G, Bauer P, Bechtold P, Beljaars ACM, van de Berg L, Bidlot J, Bormann N, Delsol C, Dragani R, Fuentesn M, Geer AJ, Haimberger L, Healy SB, Hersbach H, H'olm EV, Isaksen L, Kållberg P, Köhler M, Matricardi M, McNally AP, Monge-Sanz BM, Morcrette JJ, Park BK, Peubey C, de Rosnay P, Tavolato C, Thépaut JN, Vitart F. 2011. The ERA-Interim reanalysis: configuration and performance of the data assimilation system. *Quarterly Journal of the Royal Meteorological Society* **137**: 553–597.

Doms G, Forstner F, Heis E, Herzog HJ, Raschendorfer M, Reinhardt T, Ritter B, Schrodin R, Schulz JP, Vogel G. 2011. A Description of the Nonhydrostatic Regional COSMO Model Part II: Physical Parameterization. Technical Report September.

Fosser G, Khodayar S, Berg P. 2014. Benefit of convection permitting climate model simulations in the representation of convective precipitation. *Climate Dynamics* **44**: 45–60.

Hazeleger W, Wang X, Severijns C, Ştefănescu S, Bintanja R, Sterl A, Wyser K, Semmler T, Yang S, van den Hurk B, van Noije T, van der Linden E, van der Wiel K. 2012. EC-Earth V2: description and validation of a new seamless Earth system prediction model. *Climate Dynamics* **39**: 2611–2629.

IPCC. 2013. Summary for policymakers. Climate change 2013: the physical science basis. In *Contribution of Working Group I to the Fifth Assessment Report of the Intergovernmental Panel on Climate Change*, Stocker TF, Qin D, Plattner GK, Tignor M, Allen SK, Boschung J, Nauels A, Xia Y, Bex V, Midgley PM (eds). Cambridge University Press: Cambridge, UK and New York, NY.

Jones PW. 1999. First- and second-order conservative remapping schemes for grids in spherical coordinates. *Monthly Weather Review* **127**: 2204–2210, doi: 10.1175/1520-0493.

Kendon EJ, Roberts NM, Senior CA, Roberts MJ. 2012. Realism of rainfall in a very high-resolution regional climate model. *Journal of Climate* **25**(17): 5791–5806.

Kendon EJ, Roberts NM, Fowler HJ, Roberts MJ, Chan SC, Senior CA. 2014. Heavier summer downpours with climate change revealed by weather forecast resolution model. *Nature Climate Change* **4**: 570–576.

Kotlarski S, Keuler K, Christensen OB, Colette A, Deque M, Gobiet A, Goergen K, Jacob D, Lüthi D, van Meijgaard E, Nikulin G, Schär C, Teichmann C, Vautard R, Warrach-Sagi K, Wulfmeyer V. 2014. Regional climate modeling on European scales: a joint standard evaluation of the EURO-CORDEX RCM ensemble. *Geoscientific Model Development* **7**(4): 1297–1333.

Mearns LO, Gutowski WJ, Jones R, Leung LY, McGinnis S, Nunes AMB, Qian Y. 2009. A regional climate change assessment program for North America. *Eos* **90**(36): 311–312.

Prein AF, Gobiet A, Suklitsch M, Truhetz H, Awan NK, Keuler K, Georgievski G. 2013. Added value of convection permitting seasonal simulations. *Climate Dynamics* **41**(9–10): 2655–2677.

Prein AF, Langhans W, Fosser G, Ferrone A, Ban N, Goergen K, Keller M, Tölle M, Gutjahr O, Feser F, Brisson E, Kollet S, Schmidli J, van Lipzig NPM, Leung R. 2015. A review on regional convection-permitting climate modeling: demonstrations, prospects, and challenges. *Reviews of Geophysics* **53**: 323–361.

Ritter B, Geleyn JF. 1992. A comprehensive radiation scheme for numerical weather prediction models with potential applications in climate simulations. *Monthly Weather Review* **120**(2): 303–325.

Rockel B, Will A, Hense A. 2008. The regional climate model COSMO-CLM (CCLM). *Meteorologische Zeitschrift* **17**(4): 347–348.

Schär C, Ban N, Fischer EM, Rajczak J, Schmidli J, Frei C, Giorgi F, Karl TR, Kendon EJ, Klein Tank AMG, O'Gorman PA, Sillmann J, Zhang X, Zwiers FW. 2016. Percentile indices for assessing changes in heavy precipitation events. *Climatic Change* **137**: 201–216, doi: 10.1007/s10584-016-1669-2.

Steppeler J, Doms G, Schättler U, Bitzer HW, Gassmann A, Damrath U, Gregoric G. 2003. Meso-gamma scale forecasts using the nonhydrostatic model LM. *Meteorology and Atmospheric Physics* **82**(1–4): 75–96.

Tabari H, Agha KA, Willems P. 2014. A perturbation approach for assessing trends in precipitation extremes across Iran. *Journal of Hydrology* **519**: 1420–1427.

Tabari H, Taye MT, Willems P. 2015. Water availability change in central Belgium for the late 21st century. *Global and Planetary Change* **131**: 115–123.

Tiedtke M. 1989. A comprehensive mass flux scheme for cumulus parameterization in large-scale models. *Monthly Weather Review* **117**(8): 1779–1800.

Wagner S, Berg P, Schädler G, Kunstmann H. 2013. High resolution regional climate model simulations for Germany: part II – projected climate changes. *Climate Dynamics* **40**: 415–427.

Walther A, Jeong JH, Nikulin G, Jones C, Chen D. 2013. Evaluation of the warm season diurnal cycle of precipitation over Sweden simulated by the Rossby Centre regional climate model RCA3. *Atmospheric Research* **119**: 131–139.

Weisman ML, Skamarock WC, Klemp JB. 1997. The resolution dependence of explicitly modeled convective systems. *Monthly Weather Review* **125**(4): 527–548.

Wicker LJ, Skamarock WC. 2002. Time-splitting methods for elastic models using forward time schemes. *Monthly Weather Review* **130**(8): 2088–2097.

Willems P, Olsson J, Arnbjerg-Nielsen K, Beecham S, Pathirana A, Gregersen IB, Madsen H, Nguyen VTV. 2012. *Impacts of Climate Change on Rainfall Extremes and Urban Drainage*. IWA Publishing: London.